A Highly Selective Charge Transfer Fluoroionophore for Cu^{2+}

Zhen-Chang Wen, Rui Yang, Hui He and Yun-Bao Jiang*

Department of Chemistry and the MOE Key Laboratory of Analytical Sciences,
Xiamen University, Xiamen 361005, China and College of Chemistry and Chemical Engineering,
Southwest University, Chongqing 410075, China
ybjiang@xmu.edu.cn Tel/Fax: +86 592 2185662

Electronic Supporting Information

1. Experimental Procedures

^{1}H NMR and ^{13}C NMR were acquired in DMSO-d_6 on Varian Unity$^+$ 500MHz NMR spectrometer using TMS as an internal standard. HRMS were obtained on a Micromass LCT spectrometer by injection of methanol solution of the sample. Absorption and fluorescence spectra were recorded on Varian Cary 300 absorption spectrophotometer and Hitachi F-4500 fluorescence spectrophotometer, respectively. Solutions were measured in 1.00 cm quartz cell. The solvents employed for titration were redistilled acetonitrile (ACN) and deionized water. Fluorescence quantum yields were measured using quinine sulfate as the standard (0.546 in 0.5 mol L^{-1} H_2SO_4).[1]

All spectral titrations were carried out by keeping the sensor concentration constant while varying the concentration of metal ion. Metal ions were used as their perchlorates except Ag^+, Al^{3+}, Co^{2+} and Fe^{3+} that existed as nitrates. In the pH titration experiments, pH values of the solutions were adjusted with tetrabutylammonium hydroxide and perchloric acid solution that contained the same concentration of the metal ion.

The dipole moment of the CT state of **1** was determined as 24.1D following equation (1),[2]

$$k = \frac{\mu_1^{CT} * (\mu_1^{CT} - \mu_1^g) / \rho_1^3}{\mu_2^{CT} * (\mu_2^{CT} - \mu_2^g) / \rho_2^3} \qquad (1)$$

In (1), μ^{CT} and μ^g are the dipole moments of the CT state and the ground state, respectively. ρ is the equivalent radius of the solute and subscript numbers “1” and “2” refer to **1** and 4-dimethylaminobenzonitrile (DMABN), respectively. k is the slope of the plot in Figure S2(b). ρ_1, ρ_2 and μ_1^g were calculated as 4.95Å, 3.98Å and 6.3D, respectively, using Hartree-Fock(HF)/6-31G(d) method. μ_2^g and μ_2^{CT} of DMABN were taken as 6.6D and 16.4D from reference 2. Following the same method, the CT state dipole moment of the **1**-Cu^{2+} complex was determined as 22.6D by assuming that the dipole moment of the ground state of **1** was not changed upon binding with Cu^{2+}.

References

[1] Demas, J. N.; Crobys, G. A. *J. Phys. Chem.* **1971**, *75*, 991-1024.

[2] Zachariasse, K. A.; Grobys, M.; Tauer, E. *Chem. Phys. Lett.*, **1997**, *274*, 372-382.

2. Synthesis of **1** and **2**

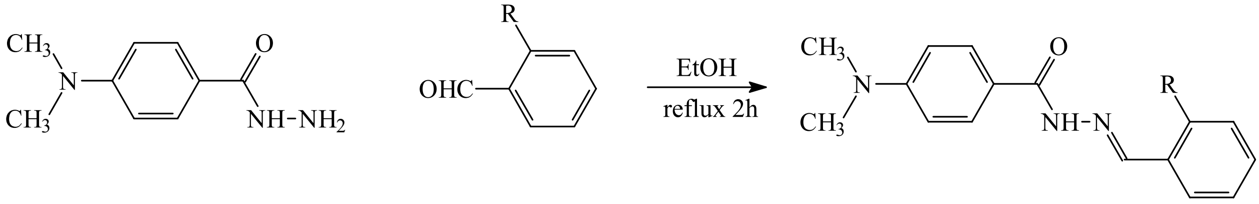

1 R = OCH_3
2: R = H

1 and its control compound **2** were synthesized by refluxing in ethanol equimolar quantities of 4-(dimethylamino)benzoylhydrazine and 2-methoxybenzaldehyde and benzaldehyde, respectively. The crude products were recrystallized from ethanol and characterized by $^{1}H/^{13}C$ NMR and HRMS.

1: ^{1}H NMR (500MHz, DMSO-d_6), δ (ppm) 2.998 (6H, s), 3.868 (3H, s), 6.748(2H, d, J = 8.5Hz), 7.018 (1H, t, J = 7.5Hz), 7.101 (1H, d, J = 8.5Hz), 7.414 (1H, t, J = 7.5Hz), 7.833 (2H, d, J = 8.5 Hz), 8.779 (1H, s), 11.557 (1H, s); ^{13}C NMR (125MHz, DMSO-d_6), δ (ppm) 40.009, 55.654, 110.811, 111.781, 119.470, 120.731, 122.720, 125.364, 129.075, 131.137, 141.543, 152.433, 157.575, 162.693. HRMS (ESI): found 298.1558; calcd for [$C_{17}H_{20}N_3O_2^+$]: 298.1556.

2: ^{1}H NMR (500MHz, DMSO-d_6), δ (ppm) 2.998 (6H, s), 6.756(2H, d, J = 9Hz), 7.400-7.647 (3H, m), 7.708 (2H, d, J = 7.5Hz), 7.817 (2H, d, J = 8.5Hz), 8.418 (1H, s), 11.558 (1H, s); ^{13}C NMR (125MHz, DMSO-d_6), δ (ppm) 39.985, 110.787, 119.422, 126.795, 128.760, 129.075, 129.675, 134.678, 146.078, 152.433, 162.818. HRMS (ESI): found 268.1448; calcd for [$C_{16}H_{18}N_3O^+$]: 268.1450.

3. Absorption spectral parameters of **1** and its metal complexes in ACN

	λ_{L}, nm	ε_{L}, 10^4 L mol^{-1} cm^{-1}	$\lambda_{L\text{-}M}$, nm	$\varepsilon_{L\text{-}M}$, 10^4 L mol^{-1} cm^{-1}	isosbestic points, nm	Binding Constant, 10^4 M^{-1} [c]
1	334	4.49	–	–	–	–
1-Fe^{3+}	334	5.50	– [b]	– [b]	–	– [b]
1-Co^{2+}	336	4.12	370	1.20	293, 342	6.98±4.31
1-Ni^{2+}	350	3.49	370	2.93	290, 350	2.15±0.29
1-Cu^{2+}	320	1.89	388	0.7	293, 363	6.64±0.81
1-Ag^{+}	334	4.99	– [b]	– [b]	–	– [b]
1-Zn^{2+}	– [a]	– [a]	370	4.30	269, 293, 348	6.52±0.37
1-Cd^{2+}	341	3.60	370	1.92	269, 293, 348	1.57±0.20
1-Hg^{2+}	– [a]	– [a]	378	3.10	278, 299, 354	25.9±25.7
1-Pb^{2+}	– [a]	– [a]	375	4.59	275, 297, 351	9.64±0.30
1-Al^{3+}	334	3.72	390	0.10	–	– [b]

a. Band peaked at 334nm disappeared. *b*. Too weak to be determined. *c*. Binding constant was fitted via a nonlinear equation assuming a 1:1 binding stoichiometry. Nice fitting supported the 1:1 stioichiometry.

4. Absorption spectra of **1** in ACN in the presence of individual metal ion

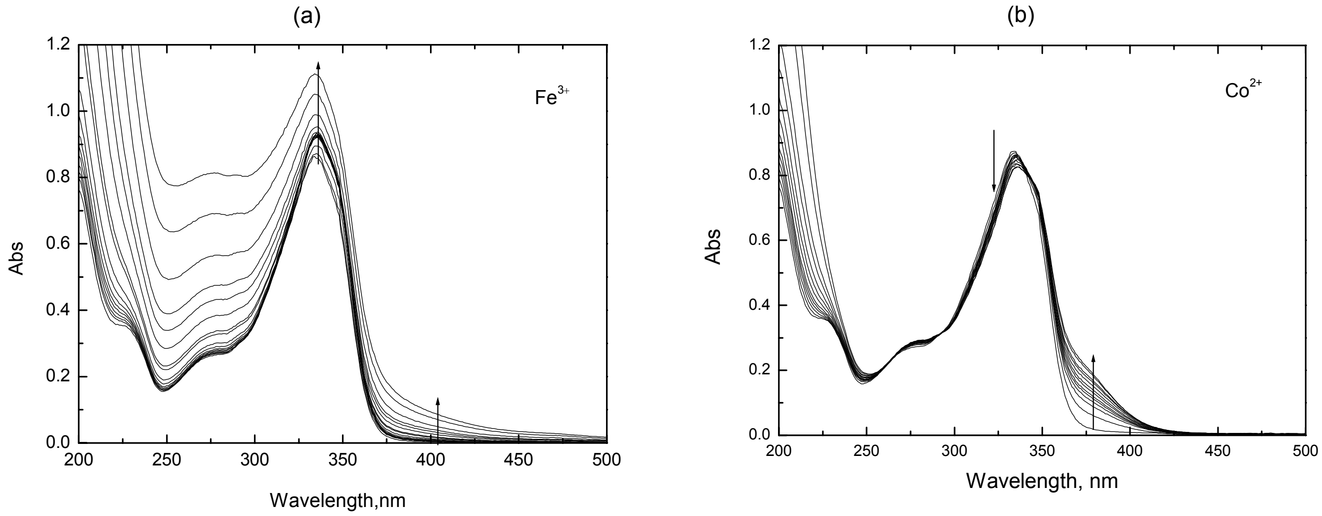

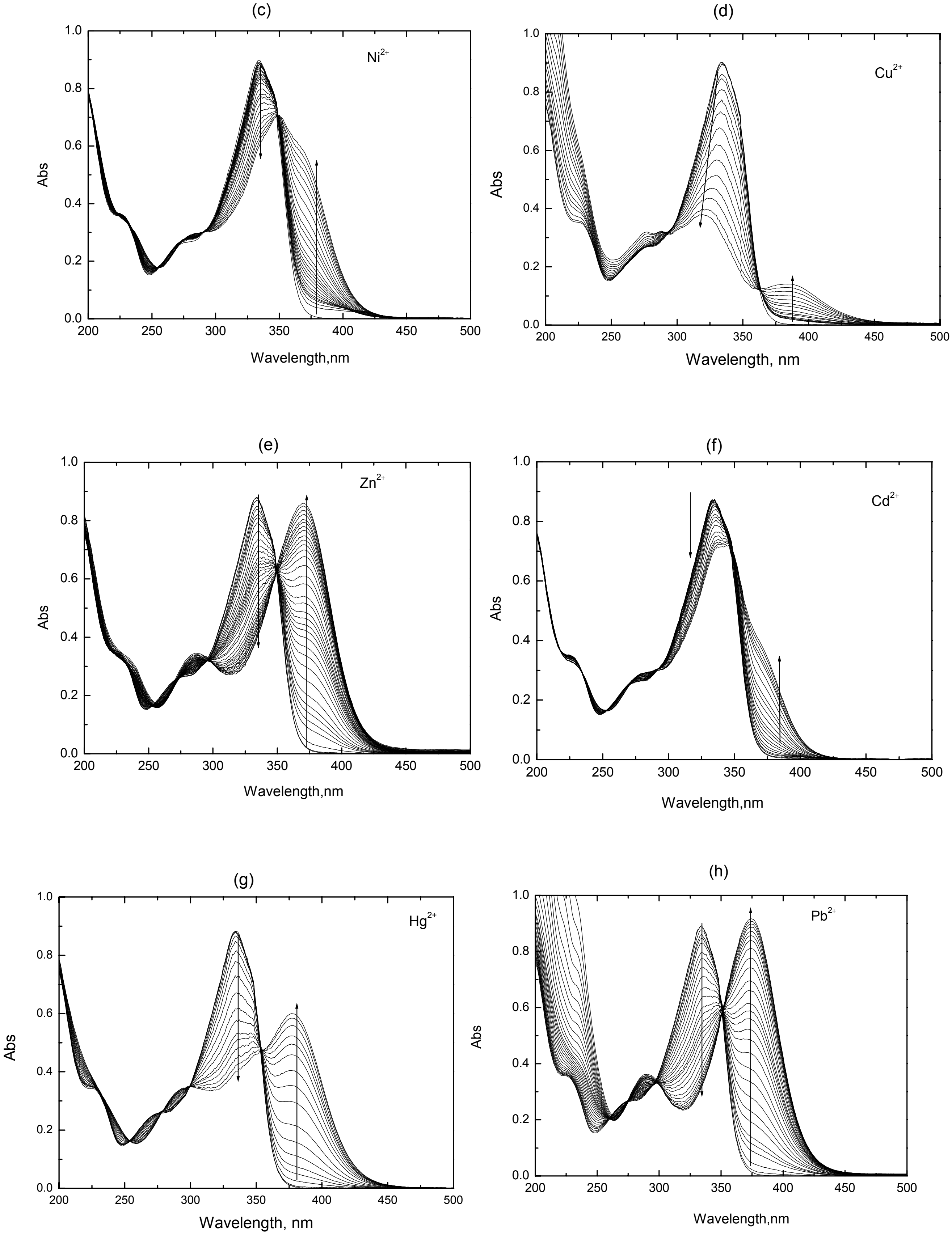
(c)
Ni^{2+}
Abs
Wavelength,nm
(d)
Cu^{2+}
Abs
Wavelength, nm
(e)
Zn^{2+}
Abs
Wavelength,nm
(f)
Cd^{2+}
Abs
Wavelength,nm
(g)
Hg^{2+}
Abs
Wavelength, nm
(h)
Pb^{2+}
Abs
Wavelength,nm
0.0
0.2
0.4
0.6
0.8
1.0
200
250
300
350
400
450
500

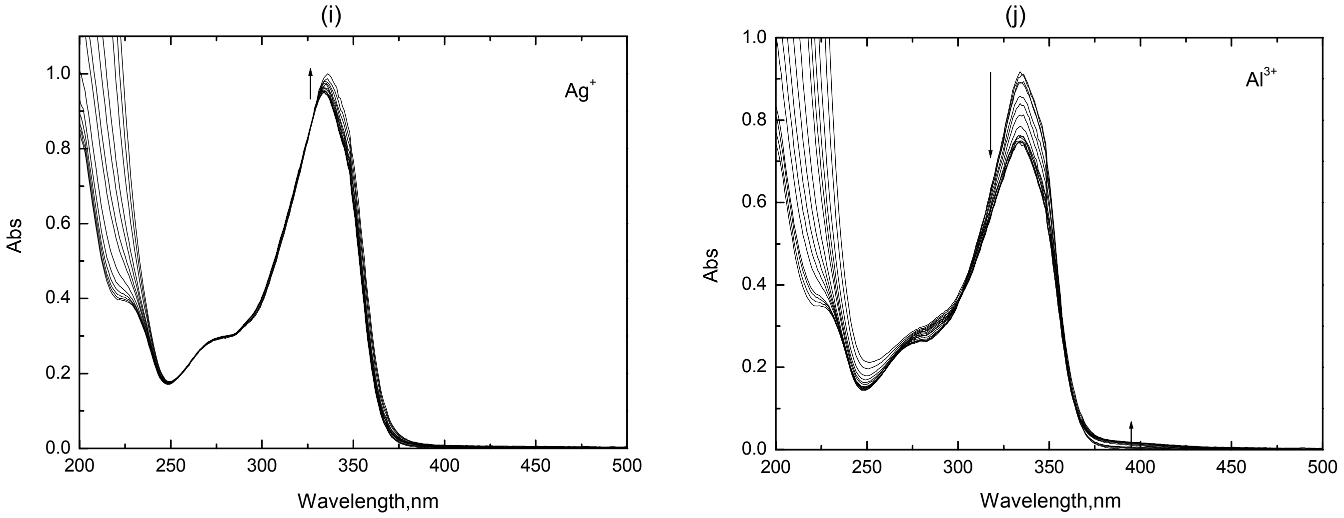

Figure S1: Absorption spectra of **1** (2.0×10^{-5} M) in ACN in the presence of increasing concentration of metal ion. Metal ions are, from (a) to (j), Fe^{3+}, Co^{2+}, Ni^{2+}, Cu^{2+}, Zn^{2+}, Cd^{2+}, Hg^{2+}, Pb^{2+}, Ag^+ and Al^{3+}, respectively.

5. Solvent effect on the fluorescence emission of **1**

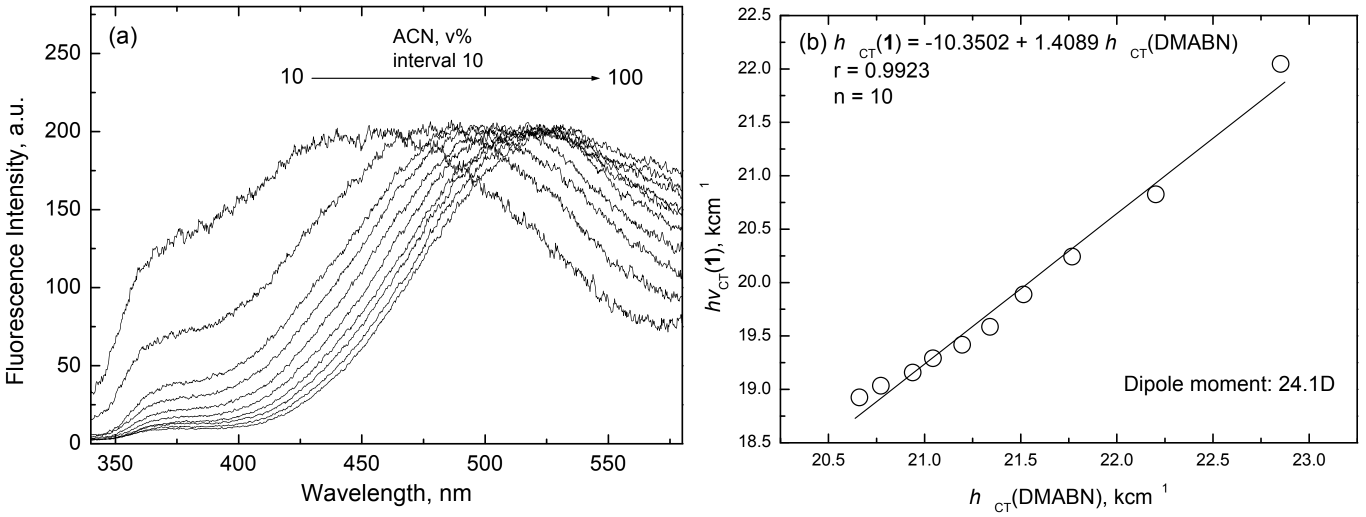

Figure S2: (a) The CT emission normalized fluorescence spectra of **1** in diethyl ether-ACN binary solvents of varied composition. [**1**] = 2.0×10^{-5} M, the excitation wavelength was 298nm. (b) Plot of the CT emission energy $h\nu^{max}$ of **1** against that of DMABN in diethyl ether-ACN binary solvents.

6. Fluorescence titration of **1** with Cu^{2+} and other transition metal ions in pure ACN

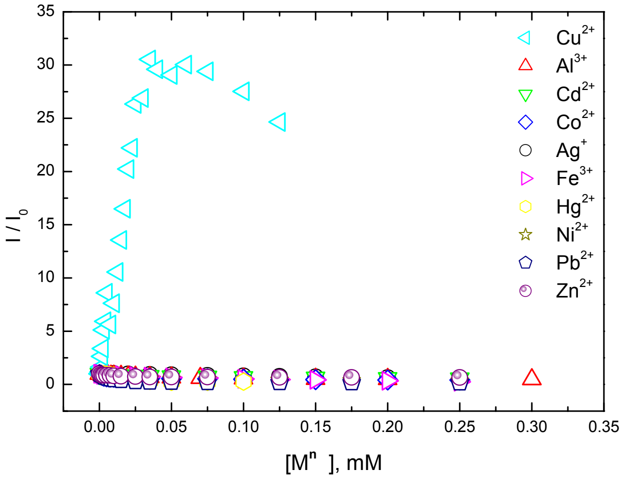

Figure S3: Plot of the fluorescence enhancement factor (I/I_0) versus concentrations of Cu^{2+} and other metal ions.

7. Fluorescence spectra of 1 in ACN-H_2O solution

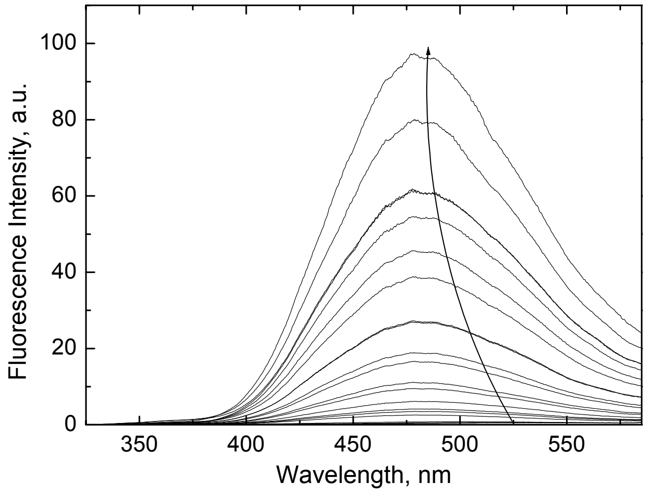

Figure S4: (a) Fluorescence spectra of **1** (2.0×10^{-5} M) in a mixture (9:1, v/v) of ACN and tris-HCl (0.005M, pH 7.2) aqueous buffer solution in the presence of increasing concentration of Cu^{2+}.

8. Fluorescence spectral parameters of **1** and **1**-Cu^{2+} in ACN and ACN-H_2O solutions

	1			**1**-Cu^{2+}		
	λ_{CT}, nm [a]	λ_{LE}, nm [b]	Φ_f [c]	λ_{CT}, nm [a]	λ_{LE}, nm [b]	Φ_f [c]
ACN	525	370	0.0082	460	370	0.28
10% H_2O	530	370	0.0020	482	370	0.32
30% H_2O	–	370	0.0015	492	375	0.23
50% H_2O	–	370	0.0014	500	375	0.16
80% H_2O	–	370	0.0007	513	375	0.042
90% H_2O	–	370	0.0004	526	380	0.016

a. The charge transfer (CT) band position. *b*. The LE band position. *c*. Total fluorescence quantum yield.

9. Solvent effect on the fluorescence emission of **1**-Cu^{2+} complex

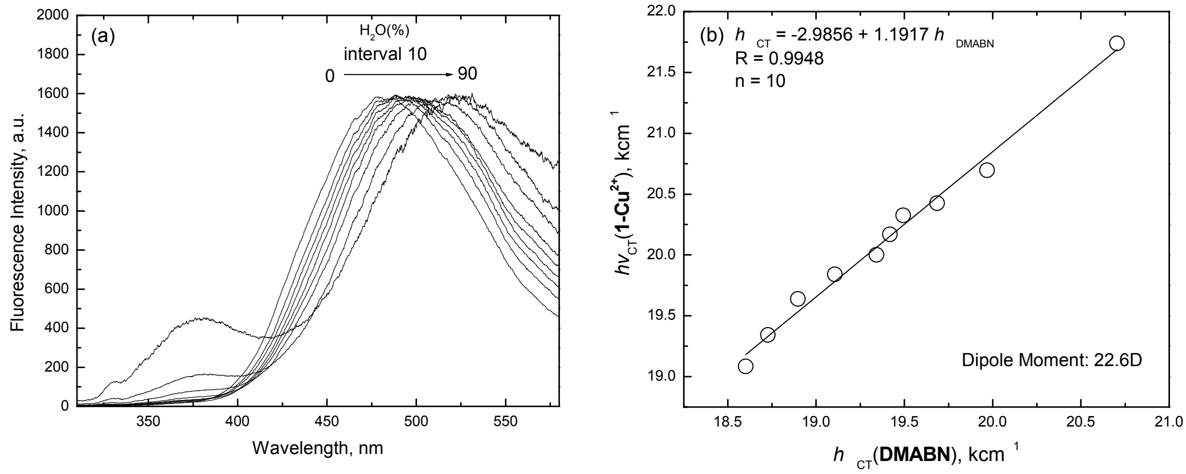

Figure S5: (a) The CT emission normalized fluorescence spectra of **1** in ACN-H_2O binary solvents in the presence of 1 equiv of Cu^{2+} and (b) plot of the CT emission energy $h\nu^{max}$ of **1**-Cu^{2+} complex against that of DMABN in ACN-H_2O binary solvents.

10. pH profiles of the fluorescence intensity of **1** in the absence and presence of Cu^{2+}

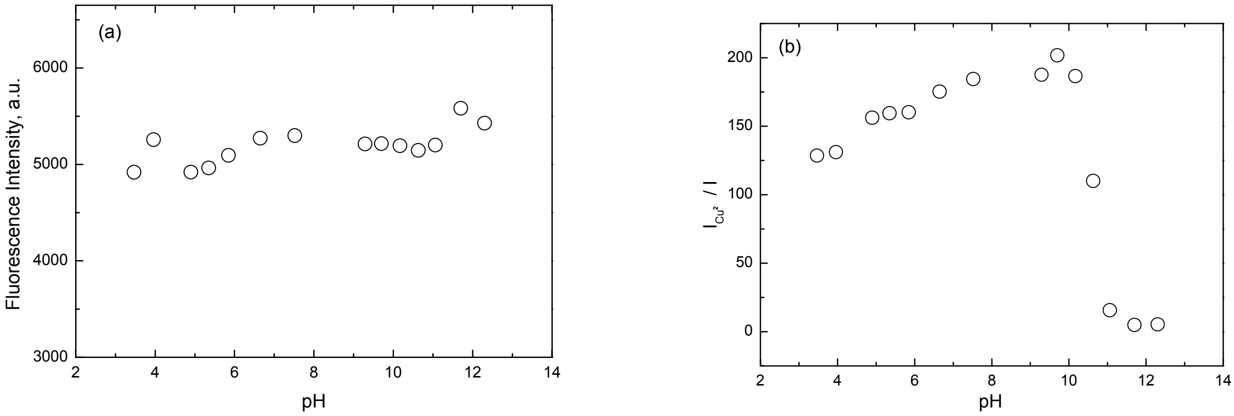

Figure S6: (a) Plot of the fluorescence intensity of **1** (2.0×10^{-5} M) and (b) fluorescence enhancement factor of **1** in the presence of 2.5 equiv of Cu^{2+} as a function of pH in ACN-H_2O (9:1, v/v) solutions.

11. ESI-MS spectrum of **1** in ACN in the presence of $Cu(ClO_4)_2$

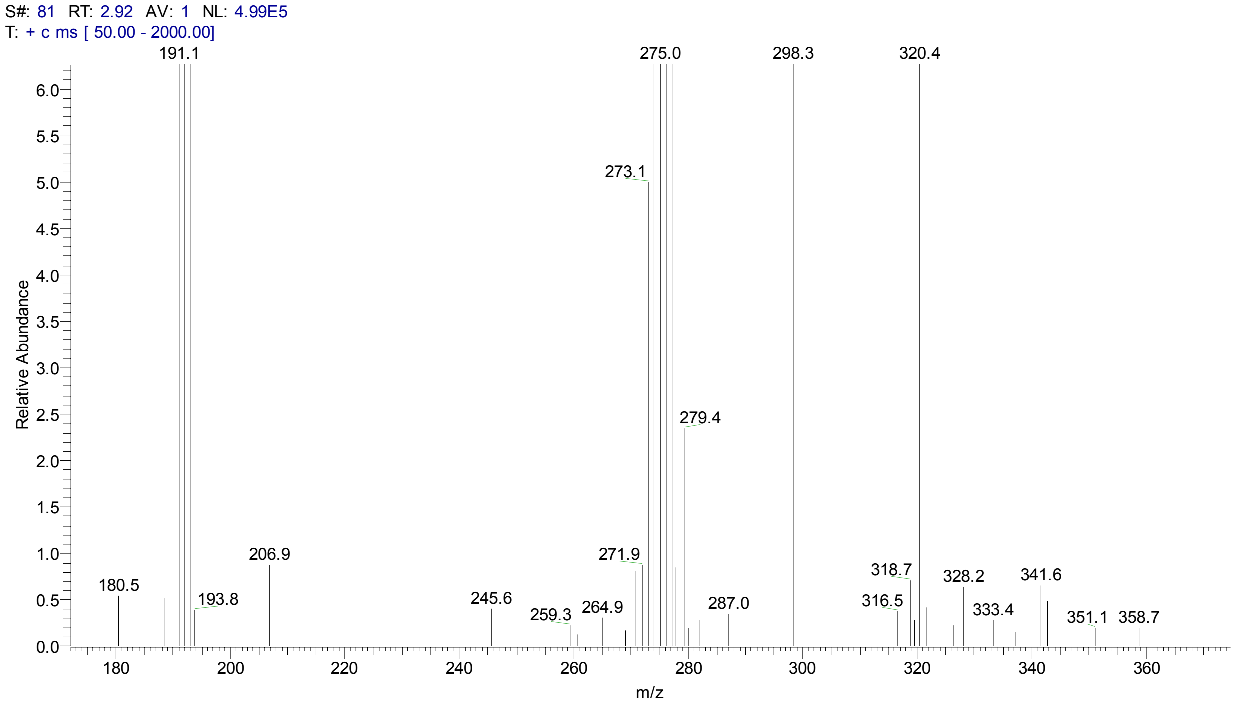

Figure S7: ESI-MS spectrum of **1** and its complex with Cu^{2+} in CAN. Peak *m/z* 180.5 corresponds to ($\mathbf{1}$+Cu^{2+})/2 and peak *m/z* 298.3 corresponds to ($\mathbf{1}$+H^+).

12. IR spectra of **1** and **1**-Cu^{2+} complex

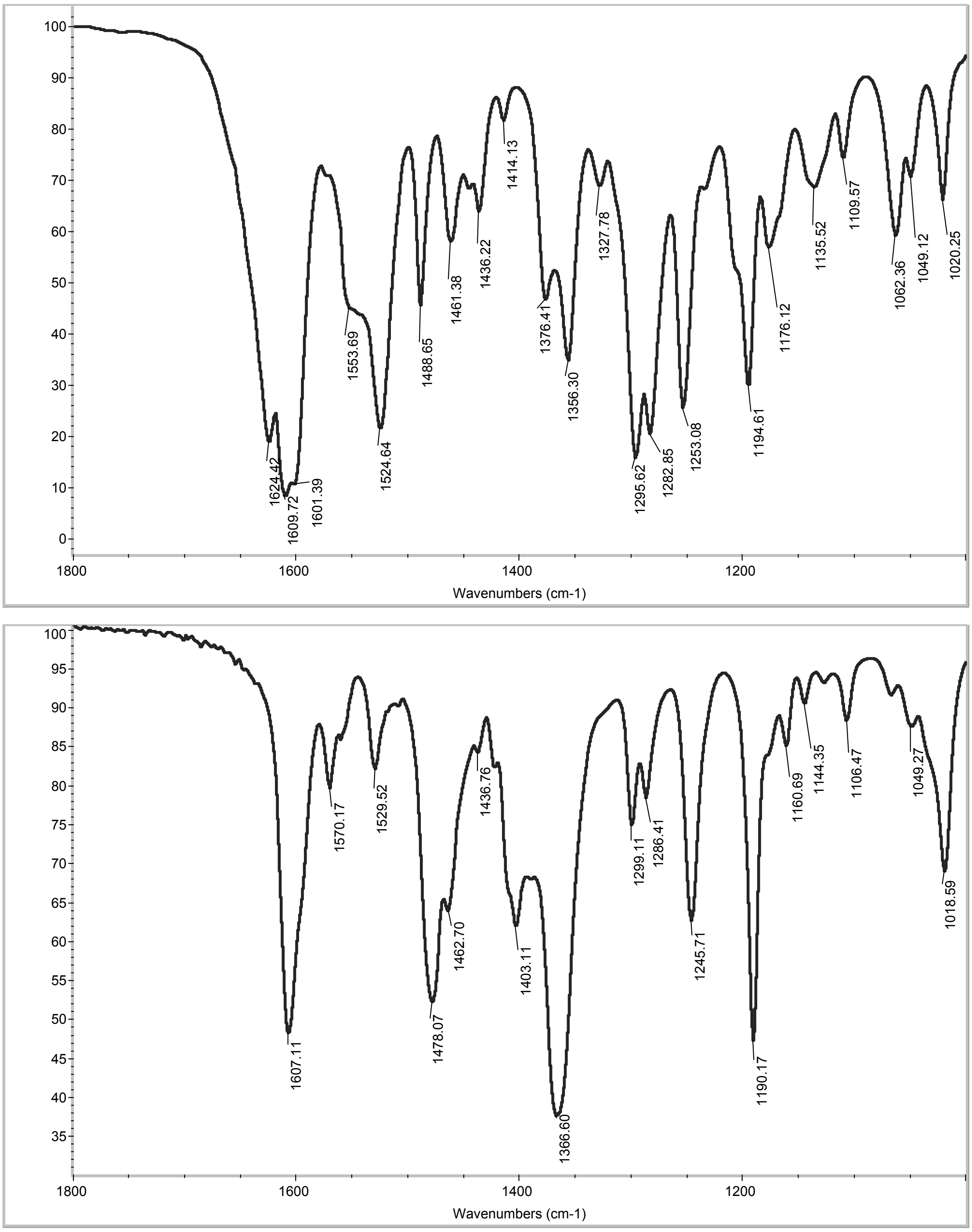

Figure S8: Partial IR spectra of **1** (top) and **1**-Cu^{2+} complex (bottom). Note that the peaks at 1624, 1609 and 1253 cm^{-1}, ascribed to C=O, C=N and C-O stretching of **1** respectively, shift upon binding to Cu^{2+} to lower wavenumber of 1609, 1570 and 1245 cm^{-1} respectively.

13. Fluorescence titration of **2** with Cu^{2+} in ACN

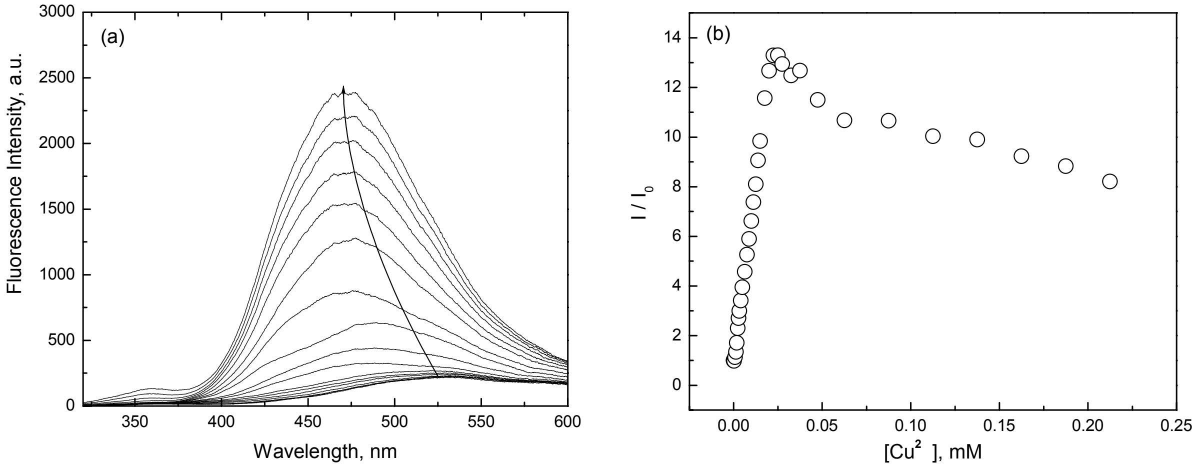

Figure S9: (a) Fluorescence spectra of **2** (2.0×10^{-5} M) in ACN in the presence of increasing concentration of Cu^{2+}. The excitation wavelength was 306 nm, the isosbestic wavelength observed in the absorption spectral titration. (b) Plot of the fluorescence enhancement factor (I/I$_0$) versus Cu^{2+} concentration. I and I$_0$ are the fluorescence intensity of **2** in the presence and absence of Cu^{2+}, respectively.

15. Fluorescence spectra in acetonitrile of **2**, **2**-Cu^{2+} complex and *N'*-isopropyl 4-(*N*,*N*-dimethylaminobenzamide (**3**)

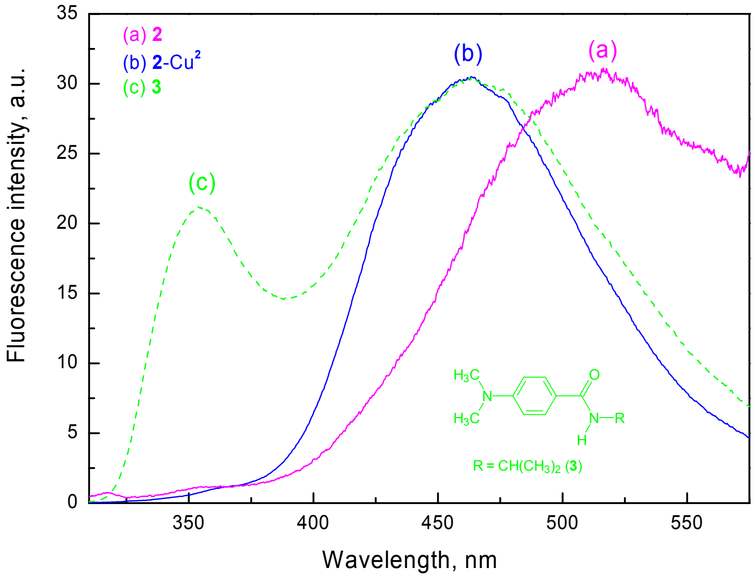

Figure S10: Fluorescence spectra in acetonitrile of **2**, **2**-Cu^{2+} complex and **3**